

# Quantum approaches to music cognition

Peter beim Graben<sup>a,\*</sup>, Reinhard Blutner<sup>b</sup>

<sup>a</sup>*Brandenburgische Technische Universität Cottbus – Senftenberg,  
Institute of Electronics and Information Technology,  
Department of Communications Engineering,  
Cottbus, Germany*

<sup>b</sup>*Emeritus Universiteit van Amsterdam,  
ILLC,  
Amsterdam, Netherlands*

---

## Abstract

Quantum cognition emerged as an important discipline of mathematical psychology during the last two decades. Using abstract analogies between mental phenomena and the formal framework of physical quantum theory, quantum cognition demonstrated its ability to resolve several puzzles from cognitive psychology. Until now, quantum cognition essentially exploited ideas from projective (Hilbert space) geometry, such as quantum probability or quantum similarity. However, many powerful tools provided by physical quantum theory, e.g., symmetry groups have not been utilized in the field of quantum cognition research so far. Inspired by seminal work by Guerino Mazzola on the symmetries of tonal music, our study aims at elucidating and reconciling static and dynamic tonal attraction phenomena in music psychology within the quantum cognition framework. Based on the fundamental principles of octave equivalence, fifth similarity and transposition symmetry of tonal music that are reflected by the structure of the circle of fifths, we develop different wave function descriptions over this underlying tonal space. We present quantum models for static and dynamic tonal attraction and compare them with traditional computational models in musicology. Our

---

\*Corresponding author

*Email address:* `peter.beimgraben@b-tu.de` (Peter beim Graben)

approach replicates and also improves predictions based on symbolic models of music perception.

*Keywords:* music psychology, tonal attraction, quantum cognition, tonal space

---

*Highlights.*

- Quantum models for tonal attraction are compared with symbolic models in musicology
- Symbolic models of tonal attraction are parsimoniously derived from fundamental symmetries of music cognition
- Tones appear as Gestalts, i.e. wave fields over the circle of fifths

## 1. Introduction

Tonal attraction is an important concept in music cognition. It refers to the idea that melodic or voice-leading pitches tend toward other pitches in greater or lesser degrees, and has been empirically investigated by means of *probe tone experiments* (Krumhansl and Shepard 1979, Krumhansl 1979). This paradigm can be regarded as a priming experiment in music psychology: In each trial, a subject is presented with a priming context (e.g. a scale, a chord, or a cadence) that establishes a tonal key, say, C major, which is followed by a probe tone randomly chosen from the twelve tones of the chromatic scale (see Sect. 2.1 for details). Subjects are then asked to rate the amount of attraction exerted by the priming context upon the probe tone. Depending on the instruction, one can distinguish between probe tone experiments on static or dynamic attraction (Parncutt 2011). In the static attraction paradigm subjects are asked to rate *how well the probe tone fits into* the preceding context (Krumhansl and Kessler 1982), while in the dynamic attraction paradigm subjects are asked to rate *how well the probe tone completes or resolves* the preceding context (Temperley 2008, Woolhouse 2009).

The difference between these different instructions is illustrated as follows: In the static attraction experiment a C major context primes the C major key such that C (the *tonic*) as a probe tone receives maximal attraction, followed by the members of the tonic triad G (the *dominant*) and E (the *mediant*). By contrast, in the dynamic attraction experiment a C major context primes the F major key because the chord CEG is the dominant triad of F major which is resolved by its tonic triad FAC, making the probe tone F most likely, followed by C and then A (Woolhouse 2009). Yet another possibility could be melodic progression where C primes its minor and major second intervals below and above, i.e. B and D within the C major scale according to the principle of *pitch proximity* (Temperley 2008).

There are essentially two research lines for computational models of tonal attraction data. The first, psychoacoustic bottom-up models are inspired by Hermann von Helmholtz' (1877) attempts on spectral representations and the overtone series (Milne et al. 2011, 2015, Stolzenburg 2015). The second, cognitive top-down models go back to Lerdahl and Jackendoff's (1983) generative theory of tonal music, using either hierarchically structured representations of tonal space (Lerdahl 1988, 1996, Krumhansl and Kessler 1982, Krumhansl and Cuddy 2010) or statistical correlations in large music corpora that are modeled by probabilistic approaches, such as Gaussian Markov chains (Temperley 2007, 2008).

This study aims at integrating structural and probabilistic theories of computational music theory into a unified framework. On the one hand, structural accounts such as the generative theory of tonal music are guided by principle musicological insights about the intrinsic symmetries of Western tonal music (Balzano 1980, Lerdahl and Jackendoff 1983, Lerdahl 1988, 1996). On the other hand, probabilistic accounts such as Bayesian models or Gaussian Markov chains are able to describe melodic progression through statistical correlations in large music corpora (Temperley 2007, 2008). Here, we apply the framework of quantum cognition (Pothos and Busemeyer 2013, Busemeyer and Bruza 2012) to music cognition in order to unify symmetry and (quantum) probability in a single framework for data from static and dynamic attraction experiments.

The paper is structured as follows: In the next section 2 we present, after a brief recapitulation of the essential concepts of music theory, two

tonal attraction experiments of Krumhansl and Kessler (1982) on static attraction and of Woolhouse (2009) on dynamic attraction. Section 3 reports our theory for modeling these results. For the static attraction data we first review the classical hierarchical models of tonal space (Lerdahl 1988, 1996, Krumhansl and Kessler 1982, Krumhansl and Cuddy 2010) (for other models, cf. Temperley (2007, 2008), Stolzenburg (2015)). Second, we present two quantum models based on the essential symmetries of the chromatic octave. Also for the dynamic attraction data, we first review one particular model of tonal space, the interval cycle model of Woolhouse (2009) and Woolhouse and Cross (2010). Guided by this approach we subsequently develop our quantum model for dynamical attraction analogous to the static case. The following section 4 presents the results of our quantum models and of the canonical models for comparison. The paper closes with a discussion and a short conclusion of our main findings.

## 2. Material and methods

As this study is devoted to symmetries in quantum models of static and dynamic tonal attraction, we first give a brief introduction into mathematical musicology (Balzano 1980, Mazzola 1990, 2002, Mazzola et al. 2016).

### 2.1. Elements of music

It is well known since Hermann von Helmholtz’ (1877) groundbreaking studies that the human auditory system cannot distinguish between acoustic stimuli with pitch frequencies  $f_0, f_1$  when their frequency ratios are separated by one octave:  $f_1/f_0 = 2$ . This fundamental *principle of octave equivalence* induces an equivalence relation of acoustic stimuli into *pitch classes*, or *chroma* (Parncutt 2011) which circularly wind up throughout different octaves. Western and also Chinese music divides this continuous pitch class circle into twelve distinguished tones, or *degrees* (Mazzola et al. 2016), comprising the chromatic scale shown in Tab. 1.

interval $j$	0	1	2	3	4	5	6	7	8	9	10	11	12
tone	C	C $\sharp$	D	E $\flat$	E	F	F $\sharp$	G	A $\flat$	A	B $\flat$	B	C’

Table 1: Pitch classes as chromatic scale degrees.

While pitch frequencies  $f_0, f_1$  appear equivalent, when they are separated by one octave, i.e.  $f_1 = 2f_0$  is the first overtone of the fundamental frequency  $f_0$ , the second overtone  $f_2 = 3f_0$  and the first one  $f_1$  yet sound similar as they are separated by a perfect fifth  $f_2/f_1 = 3/2$ . This auditory *principle of fifth similarity* lead to the historic development of the *diatonic scales* of Western tonal music (v. Helmholtz 1877, Schönberg 1978). In diatonic scales seven tones are arranged in a particular order of full-tone (major second) and semitone (minor second) steps. For the key of C major, these are the seven tones in ascending order C, D, E, F, G, A, B, C', namely the white keys of a piano keyboard with C' closing the octave. The tonic C is regarded as the most stable note. The same tones arranged after cyclic permutation, A, B, C, D, E, F, G, A', entail the *relative minor* scale of (natural) A minor with tonic A.

Figure 1(a) presents the chroma circle (Krumhansl 1979) consisting of the twelve circularly repeating pitch classes of the chromatic scale in equal temperament, together with the C major scale degrees depicted as open bullets. The tonic C is indicated by  $j = 0$ . The relative A minor scale is obtained by rotating all tones 3 semitone steps (i.e. a minor third) in clockwise direction, thus assigning A to  $j = 0$ . The particular order: 2, 2, 1, 2, 2, 2, 1 of major second (2 steps) and minor second (1 step) intervals characterizes all major scale modes, while (natural) A minor is characterized by the interval order 2, 1, 2, 2, 1, 2, 2, as every other minor scale mode, too. Hence, the *parallel minor* scale of C major is (natural) C minor, comprising C, D, Eb, F, G, Ab, Bb, C' with tonic C.

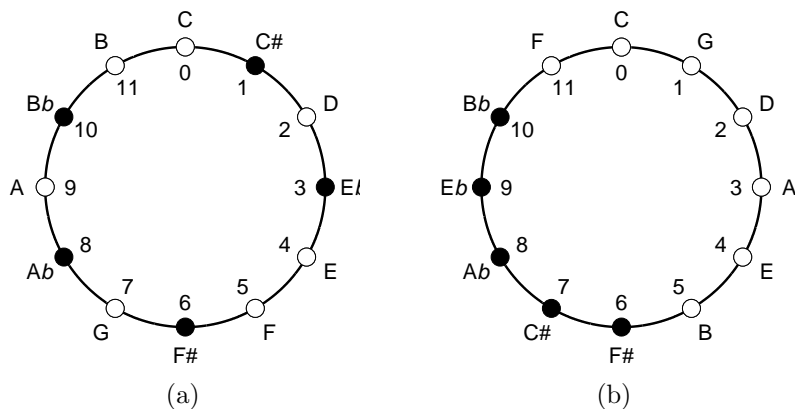


Figure 1: Tonal spaces of Western music. (a) Chroma circle of C major scale. (b) Circle of fifths. Open bullets indicate scale (diatonic) tones; closed bullets denote non-scale (chromatic) tones.

The chroma circle Fig. 1(a) exhibits the geometric symmetry of a dodecagon, corresponding to the cyclic group of integer cosets modulo twelve,  $\mathbb{Z}_{12}$  (Balzano 1980, Mazzola et al. 2016), that is generated by the semitone step  $g \in \mathbb{Z}_{12}$  through its powers  $g, g^2, g^3, \dots, g^{11}, g^{12}$  with  $g^{12} = e$  as the neutral element of the group. Hence, the inverse of an element  $g^k$  is given as  $g^{12-k}$  with  $g^6$  as its own inverse, i.e.  $g^6$  is nilpotent. The application of the generator  $g \in \mathbb{Z}_{12}$  to the chroma circle corresponds to a clockwise transposition by one semitone in Fig. 1(a).

The cyclic group  $\mathbb{Z}_{12}$  does not only possess the fundamental generator  $g$ . Yet all (integer) powers of  $g$  that are relatively prime with the group order  $n = 12$  are generators as well. Therefore, we obtain all generators of  $\mathbb{Z}_{12}$  as  $G_{12} = \{g, g^5, g^7, g^{11}\}$ . As  $g$  corresponds to one semitone step in clockwise direction around the chroma circle, its inverse  $g^{11} = g^{12-1}$  denotes one semitone step in counterclockwise direction. Similarly,  $g^7$  in clockwise direction is inverse to  $g^5$  in counterclockwise direction. Iterating the generator  $g^7$  in clockwise direction to Fig. 1(a), i.e. by applying powers of  $(g^7)^m$  to the tonic, yields the important *circle of fifths*, shown in Fig. 1(b), where all diatonic degrees are accumulated in a connected set (Balzano 1980). With the tonic of C major in position  $j = 0$ , its *dominant* G is in position  $j = 1$ , and its *sub-dominant* F is in position  $j = 11$ . The circle of fifths [Fig. 1(b)] reflects both fundamental principles of auditory pitch perception: octave equivalence is in-

icated by the identity  $g^{12} = e$ , whereas fifth similarity becomes geometrical neighborhood: two tones  $(g^7)^m, (g^7)^n$  are the more similar the smaller  $n - m \bmod 12$ . Alternatively, one could say that two tones are the more similar the smaller their angle along the circle of fifths. This similarity measure leads directly to our quantum model discussed in Sect. 3.1.2.

The universal symmetry in tonal music is *transposition invariance* (Köhler 1969): A melody does not significantly alter its character, when played in a different key. Transposition from one key into another one is carried out by rotations either along the chroma circle or along the circle of fifths. Rotating here all tones one step in clockwise direction, assigns  $j = 0$  to F which thereby becomes the tonic of F major with dominant  $j = 1$  at C and subdominant  $j = 11$  at Bb. Correspondingly, G major is obtained by a counterclockwise rotation by one step with tonic G ( $j = 0$ ), dominant D ( $j = 1$ ), and subdominant C ( $j = 11$ ).

These are only a few examples for symmetries of the chroma circle. Others are the dichotomy between consonances and dissonances (v. Helmholtz 1877, Mazzola et al. 2016), or the emergence of the *third torus* as the direct group product  $\mathbb{Z}_{12} = \mathbb{Z}_3 \times \mathbb{Z}_4$  (Balzano 1980, Mazzola et al. 2016) which is crucial for the canonical construction of tertian chords in harmony theory (Schönberg 1978). This decomposition maps both, the chroma circle and the circle of fifths onto a torus, generated by a minor third (3 steps) in one direction and a major third (4 steps) in the orthogonal direction. Starting with C and going 4 steps, yields E, from where one arrives at G after 3 orthogonal steps, thus forming the C major triad CEG. Iterating first 3 and then 4 steps, instead, entails the C minor triad C**E**bG. Likewise, the F major triad is comprised by its tonic F, its major third, A, and the minor third C of A. For G major, one obtains correspondingly G**B**D.

## 2.2. Static tonal attraction

In a celebrated probe tone experiment on static tonal attraction, Krumhansl and Kessler (1982) asked musically experienced listeners to rate how well, on a seven point scale, each note of the chromatic octave fitted with a preceding context, which consisted of short musical sequences, such as ascending scales, chords, or cadences, in major or minor keys. All stimuli were prepared as artificial

Shepard tones (Krumhansl and Kessler 1982, Woolhouse 2009, Milne et al. 2015), i.e. superpositions of pure sinusoids over five octaves with Gaussian amplitude envelopes.

The empirical results of Krumhansl and Kessler (1982) are replicated in Fig. 2 as dotted curves connecting open and closed bullets. The probe tones are given as physical pitch frequencies (in Hz) at the  $x$ -axis. The subjective attraction ratings  $A_{KK}(x)$  (referring to Krumhansl and Kessler) are plotted at the  $y$ -axis. Figure 2(a) shows the results for the C major context, and Fig. 2(b) for the C minor context. The results of this experiment clearly show a kind of hierarchy: all diatonic scale tones (open bullets) received higher ratings than the chromatic nonscale tones (closed bullets). Moreover, in both modes, C major and C minor, the tonic C is mostly attractive, followed by the fifth, G and the third E for C major [2(a)] and by the third Eb and then the fifth G for C minor [2(b)].

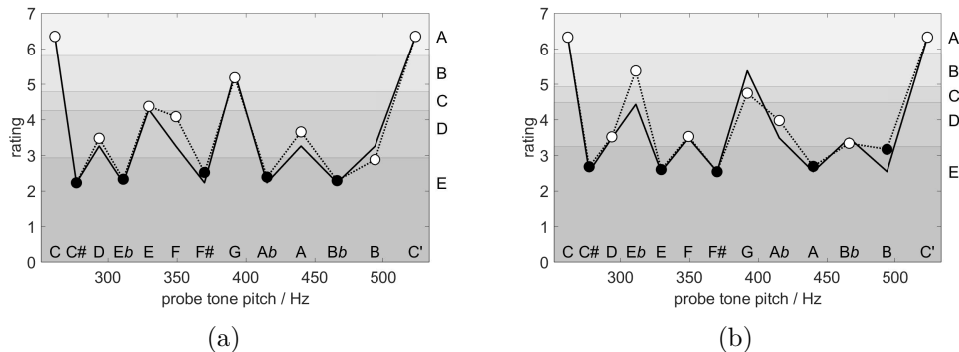


Figure 2: Static tonal attraction. Dotted with bullets: rating data  $A_{KK}(x)$  of Krumhansl and Kessler (1982) against physical pitch frequency  $f$  in Hz, solid: predictions from the hierarchical model [Eq. (1)]. The labels A – E at the right hand side indicate the labels of the hierarchical model [Tab. 2]. (a) For C major context. (b) For C minor context. Open bullets indicate scale (diatonic) tones; closed bullets denote non-scale (chromatic) tones, for the respective scale.

Carrying out a multiscale analysis of their behavioral data, Krumhansl and Kessler (1982) recovered a geometric representation of keys akin to the third torus, thereby supporting the hierarchical models of tonal space as discussed in Sect. 3.1.1 (Lerdahl 1988, 1996, Krumhansl and Kessler 1982, Krumhansl and Cuddy 2010). We additionally present the predictions of the hierarchical model as

the solid curves together with the labels of its levels in Fig. 2.

### 2.3. Dynamic tonal attraction

Using five different chords, also consisting of Shepard tones, the C major triad CEG, the C minor triad CE♭G, the dominant seventh CEGB♭, a French sixth CEG♭B♭, and a half-diminished seventh CE♭G♭B♭, as contexts, Woolhouse (2009) conducted a dynamic attraction probe tone experiment, asking listeners, how well a chromatic probe tone was melodically completing or harmonically resolving the priming context.

The results of this study are replicated in Sect. 4.2, Fig. 7 for the five contexts. The dotted curves connecting open and closed bullets present the original results of the Woolhouse (2009) experiment, where probe tones are arranged along the circle of fifths [Fig. 1(b)] as real numbers  $x = j\pi/6$  ( $j \in \mathbb{Z}_{12}$ , with  $C(0) \cong C'(12)$  one octave higher) at the  $x$ -axis.

Figure 7(a) displays the results for the C major priming context. The highest rated tone is F which is consistent with the interpretation of the priming C major triad as the dominant of F major. Another plausible interpretation of the prime would be the subdominant of G major, thus predicting higher likelihood of probe tone G. Similar results could be expected for the C minor context shown in Fig. 7(b). In fact, F receives a relatively large rating, however, outperformed by A♭. Figure 7(c) displays the dominant seventh chord which is similar to the C major triad. The data for the French sixth presented in Fig. 7(d) give highest ratings for F and B and lowest ratings for D and A♭. Finally, the half-diminished seventh [Fig. 7(e)] is most likely resolved by F, C♯ and B.

## 3. Theory

In this section we develop our quantum models of static and dynamic tonal attraction, based on the fundamental principles of octave equivalence, fifth similarity and the universal musical transposition symmetry.

### 3.1. Static tonal attraction

Before we enter into the derivation of two possible quantum models for static tonal attraction, we briefly review the influential symbolic model based on the generative theory of tonal music (Lerdahl and Jackendoff 1983).

#### 3.1.1. Hierarchical model

The hierarchical model of Lerdahl (1988, 1996), Krumhansl and Kessler (1982), and Krumhansl and Cuddy (2010), depicted in Tab. 2, comprises five levels of symbolic significance.

A: octave	C											C'	
B: fifths	C						G					C'	
C: triadic	C			E			G					C'	
D: diatonic	C		D	E	F		G		A		B	C'	
E: chromatic	C	C $\sharp$	D	E $\flat$	E	F	F $\sharp$	G	A $\flat$	A	B $\flat$	B	C'
$s(j)$	4	0	1	0	2	1	0	3	0	1	0	1	4

Table 2: Hierarchical model of static tonal attraction for C major context after Lerdahl (1996, 2015).

At the lowest, chromatic level E, all 12 tones of the chromatic octave are included. At the next, the diatonic level D, only the diatonic scale degrees are represented. One level higher, at the triadic level C, the three tones composing the triad according to major and minor third steps along the third torus are present. Again, one level higher, only tonic and fifths comprise the fifths level B. At the highest octave level A, eventually only the tonic prevails. The levels A – E are indicated in Fig. 2 as four shades of grey.

For each chromatic scale degree that serves as probe tone in the Krumhansl and Kessler (1982) experiment, one simply counts the number of degrees that are commonly shared across levels A to D (omitting level E that is common for all tones). The resulting number,  $s(j)$ , for probe tone  $j \in \mathbb{Z}_{12}$  can be related to an attraction probability (Temperley 2008)

$$p(j) = \frac{s(j)}{\sum_j s(j)} \quad (1)$$

that is rescaled and plotted in Fig. 2 above as solid lines and correlated with the Krumhansl and Kessler (1982) data in Tab. 5 in Sect. 4.1.<sup>1</sup>

The predictions of the hierarchical model are in good agreement with the experimental data. However, Fig. 2(b) indicates a slight deviation for C minor: the predicted attraction rate for the fifths G is larger and that of the minor third Eb is lower than the respective measured rate. We address this issue in section 3.1.5 below.

### 3.1.2. Free quantum model

A more instructive representation of the Krumhansl and Kessler (1982) data can be obtained by plotting the ratings  $A_{KK}(x)$  along the circle of fifths (beim Graben and Blutner 2017). This is done in Sect. 4.1, Fig. 5. Here, the probe tones are represented as real numbers  $x = j\pi/6$  ( $j \in \mathbb{Z}_{12}$ , with  $C(0) \cong C'(12)$  one octave higher) at the  $x$ -axis corresponding to the radian angles at the unit circle  $S^1 = \mathbb{R}/2\pi\mathbb{Z}$  interpreted as the circle of fifths [Fig. 1(b)]. The subjective attraction ratings  $A_{KK}(x)$  are plotted at the  $y$ -axis. Figure 5(a) shows the results for the C major context, and 5(b) for the C minor context.

The reordered rating profiles in Fig. 5 now exhibit some kind of periodicity: probe tones that are close to the tonic C ( $x = 0$ ) at the circle of fifths receive higher attraction values than tones that are close to the tritone F $\sharp$  ( $x = \pi$ ). Therefore, the tritone F $\sharp$  may be seen as “orthogonal” to the tonic C in an appropriately chosen metric (cf. Mannone and Compagno (2013), Mannone and Mazzola (2015) for alternative similarity assessments in musicology).

As a psychologically plausible model for static tonal attraction we therefore suggest the cosine similarity between the tonic context 0 and a probe

---

<sup>1</sup> For C minor we use the so-called *natural* minor scale which is obtained from the transposition of C major along the circle of fifths. There are two other minor scales, called *harmonic* and *melodic* minor which differ from natural minor in additional one or two semitone steps in ascending or descending lines.

tone  $x$ ,

$$p(x) = \cos^2 \frac{x}{2} \quad (2)$$

which directly reflects the auditory fifth similarity represented by the circle of fifths.

Cosine similarity is closely related to quantum similarity (Pothos et al. 2013, Pothos and Trueblood 2015) in the framework of quantum cognition models (Busemeyer and Bruza 2012, Pothos and Busemeyer 2013, Blutner and beim Graben 2016). Therefore, we express the attraction value  $p(x)$  through a continuous “wave function”  $\psi(x)$  upon the circle of fifths which constitutes the one-dimensional “tonal configuration space” of our quantum model.<sup>2</sup>

Quantum mechanical wave functions are particular instances of *state vectors* in quantum theory. A state vector comprises a complete description of the state of a quantum system. It is contained in a vector space, called Hilbert space, that is equipped with a scalar product, thus allowing the calculation of projections. A quantum mechanical measurement device defines an orthogonal basis, such that the projections of a given state vector onto the individual basis vectors are interpreted as probabilities of the respective measurement results. Accordingly is the similarity of two quantum states given through the projection of one vector onto the other one, i.e. their common scalar product. Moreover, rotating a state vector in abstract Hilbert space must not change its physically relevant properties, i.e. projection probabilities. Therefore such rotations appear as *symmetries* in quantum theory.

Our *free quantum model* (beim Graben and Blutner 2017) for the tonic wave function is hence

$$\psi(x) = \frac{1}{\sqrt{\pi}} \cos \frac{x}{2}. \quad (3)$$

The quantum wave function for an arbitrary context tone  $a$  is obtained by applying a transposition operator  $T_a$  to the tonic context 0 through

$$\psi_a(x) = T_a \psi(x) = \psi(x - a) \quad (4)$$

---

<sup>2</sup> Note that the unit circle  $S^1$  is a one-dimensional manifold, parameterized by a single continuous variable  $x \in [0, 2\pi[$ , that is embedded into two-dimensional Euclidian space.

for the amount  $a \in \mathbb{Z}_{12}$  rotating along the circle of fifths in clockwise direction. Applying the transposition operator to the tonic wave function (3), we obtain

$$\psi_a(x) = \frac{1}{\sqrt{\pi}} \cos \frac{x-a}{2} \quad (5)$$

which can be expanded by virtue of the trigonometric addition theorems:

$$\begin{aligned} \psi_a(x) &= \frac{1}{\sqrt{\pi}} \cos \frac{x-a}{2} \\ &= \frac{1}{\sqrt{\pi}} \cos \frac{a}{2} \cos \frac{x}{2} + \frac{1}{\sqrt{\pi}} \sin \frac{a}{2} \sin \frac{x}{2} \\ &= \frac{1}{\sqrt{\pi}} \cos \frac{a}{2} \cos \frac{x}{2} + \frac{1}{\sqrt{\pi}} \sin \frac{a}{2} \cos \frac{x-\pi}{2} \\ &= \cos \frac{a}{2} \psi_0(x) + \sin \frac{a}{2} \psi_\pi(x). \end{aligned}$$

Hence any transposed state becomes a linear combination of two basic context states, the tonic (C)  $\psi_0$ , and the orthogonal tritone (F $\sharp$ )  $\psi_\pi$ . The underlying Hilbert space of the free quantum model is therefore two-dimensional which proves the equivalence of this model with the earlier qubit model of Blutner (2015).

The family  $\{\psi_0, \psi_\pi\}$  constitutes an orthonormal basis with respect to the wave function scalar product

$$\langle \psi_y | \psi_a \rangle = \int_0^{2\pi} \psi_y(x)^* \psi_a(x) dx \quad (6)$$

where complex conjugation can be essentially neglected in the present case. Inserting the respective transposed wave functions yields

$$\begin{aligned} \langle \psi_y | \psi_a \rangle &= \left\langle \cos \frac{y}{2} \psi_0 + \sin \frac{y}{2} \psi_\pi \middle| \cos \frac{a}{2} \psi_0 + \sin \frac{a}{2} \psi_\pi \right\rangle \\ &= \cos \frac{y}{2} \cos \frac{a}{2} \langle \psi_0 | \psi_0 \rangle + \cos \frac{y}{2} \sin \frac{a}{2} \langle \psi_0 | \psi_\pi \rangle + \sin \frac{y}{2} \cos \frac{a}{2} \langle \psi_\pi | \psi_0 \rangle + \sin \frac{y}{2} \sin \frac{a}{2} \langle \psi_\pi | \psi_\pi \rangle \\ &= \cos \frac{y}{2} \cos \frac{a}{2} + \sin \frac{y}{2} \sin \frac{a}{2} \\ &= \cos \frac{y-a}{2} \end{aligned}$$

which is, up to a scaling factor,

$$\langle \psi_y | \psi_a \rangle = \sqrt{\pi} \psi(y-a), \quad (7)$$

the original wave function for the interval between probe tone  $y$  and context tone  $a$ . Therefore, we can use the (scaled) quantum probability density

$$p(x) = |\psi(x)|^2 = \psi(x)^*\psi(x) \quad (8)$$

for a given interval as a measure of tonal attraction  $p(y - a)$ .

Sofar, our wave functions yield static tonal attraction values through the projection (7) of a probe tone state onto a context tone state. In order to describe chord contexts, Woolhouse (2009), Woolhouse and Cross (2010) and Blutner (2015) suggested either to sum or to average the attraction profiles of individual pairs of tones over all pairings. For a context of two tones  $a, b$  this *Woolhouse conjecture* yields

$$p_{ab}(x) = |\psi_{ab}(x)|^2 = \frac{1}{2} (|\psi_a(x)|^2 + |\psi_b(x)|^2) , \quad (9)$$

in analogy to the density matrix formalism of statistical quantum mechanics (cf. Mannone (2018) for a related account in musicology). For an arbitrary number  $N$  of equally weighted context tones in a chord, we get

$$p_C(x) = \frac{1}{N} \sum_{i=1}^N |\psi_{a_i}(x)|^2 = \frac{1}{N} \sum_{i=1}^N |\psi(x - a_i)|^2 \quad (10)$$

with context  $C = \{a_i \in \mathbb{Z}_{12} | i = 1, \dots, N\}$ . When context tones are to be considered as differently weighted, we introduce weight factors  $\rho(a_i)$  (Mazzola 2002) and obtain a discrete convolution

$$p_C(x) = \sum_{i=1}^N \rho(a_i) p(x - a_i) \quad (11)$$

with kernel  $p(x) = |\psi(x)|^2$ .

Let us examine the behavior of the discrete convolution under transposition  $a \in \mathbb{Z}_{12}$ . Applying the linear transposition operator  $T_a$  to (11) yields

$$\begin{aligned} T_a p_C(x) &= \sum_{i=1}^N \rho(a_i) T_a p(x - a_i) = \sum_{i=1}^N \rho(a_i) p(x - a_i - a) = \\ &= \sum_{i=1}^N \rho(a_i) p(x - (a_i + a)) = \sum_{i=1}^N \rho(b_i - a) p(x - b_i) = \sum_{i=1}^N \rho(b_i) p(x - b_i) = p_{T_a C}(x), \end{aligned}$$

if the convolution weights are transposition invariant

$$\rho(b_i - a) = \rho(b_i) \tag{12}$$

under the substitution  $b_i = a_i + a$ . Therefore, discrete convolution (11) implies transposition invariance (12), or, in other words: transposition invariance is a necessary condition for the mixture of quantum states over chord contexts. This means that all context tones in a chord  $C$  become transposed by the same interval  $a \in \mathbb{Z}_{12}$ :  $T_a C = \{b_i \in \mathbb{Z}_{12} | b_i = a_i + a, i = 1, \dots, N\}$ . This is definitely the case for equally weighted contexts  $\rho(a_i) = 1/N$  used in our present exposition.<sup>3</sup> In our quantum model, tones appear hence as wave fields over the circle of fifths, or, likewise, as *Gestalts* in the sense of Köhler (1969).

### 3.1.3. Quantum deformation model

Our free quantum model from Sect. 3.1.2 demonstrates that the tonal attraction data of the Krumhansl and Kessler (1982) experiment as shown in Sect. 4.1, Fig. 5 can be described in first approximation by a psychologically motivated cosine similarity model upon the circle of fifths. The structure of this geometrically represented tonal space is universal for music cognition as resulting from the fundamental principles of octave equivalence and transposition symmetry (Lerdahl 1988, Krumhansl and Kessler 1982, Janata 2007). In this subsection, we show how a straightforward modification of the free model leads to a more parsimonious representation of tonal space than the hierarchical model discussed in Sect. 3.1.1.

To this aim, we introduce a suitable deformation (beim Graben and Blutner 2017) of the distances along the circle of fifths by making the ansatz

$$\psi(x) = A \cos(\gamma(x)) \tag{13}$$

for the stationary wave function where  $\gamma(x)$  is a spatial deformation function and  $A$  is a normalization constant.

---

<sup>3</sup> A more rigorous proof by means of harmonic analysis, which also entails the quantization of the continuous pitch spectrum into the discrete circle of fifths, will be published elsewhere.

### 3.1.4. Symmetric deformation

In a first attempt we develop a symmetric deformation model for the Krumhansl and Kessler (1982) data. As a starting point we linearly rescale the empirical data

$$A_{\text{KK}}(x) = ap(x) + b. \quad (14)$$

Inserting scaling constants  $a = A_{\text{max}} - A_{\text{min}}$ ,  $b = A_{\text{min}}$ , where  $A_{\text{min}}$  and  $A_{\text{max}}$  are the smallest and largest data values, and Eq. (13), and subsequently solving for  $\gamma$  yields

$$\gamma(x) = \arccos \sqrt{\frac{A_{\text{KK}}(x) - A_{\text{min}}}{A_{\text{max}} - A_{\text{min}}}}. \quad (15)$$

When we transform the C major data according to (15) we obtain  $\gamma(x)$  as the dotted curve in Fig. 3(a) resembling a buckled parabola (though neglecting the peak at E). Thus, we may fit the exponent  $n$  of a symmetric  $n$ -th order polynomial

$$\gamma(x) = a_0 + a_n(x - \pi)^n, \quad (16)$$

to the transformed data. For  $n = 2$  the fit is rather poor ( $r = 0.88$ ) and not really able to reproduce the buckle in the transformed data set. The next fit  $n = 4$  works considerably well ( $r = 0.96$ ), while exponents of higher than fourth order ( $n = 6, 8$ ) do not substantially improve our fits. Thus, our choice  $n = 4$  fits the data most parsimoniously.

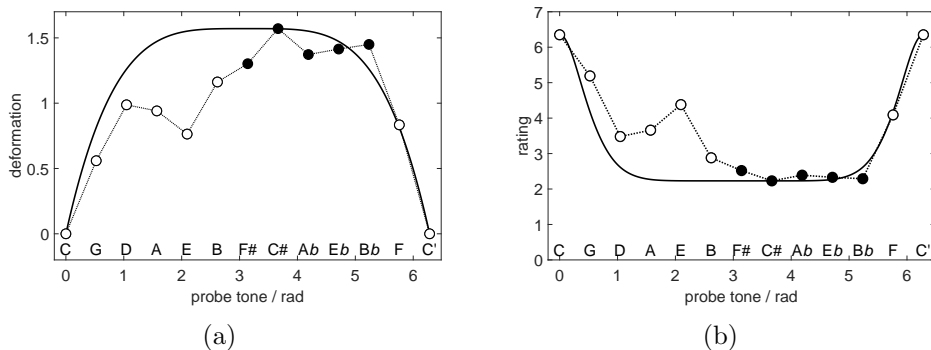


Figure 3: Optimal deformation of the cosine similarity profile for static tonal attraction. (a) Transformed Krumhansl and Kessler (1982) data [Eq. (15)] (dotted) against radian angles at the circle of fifths and deformation function (17) (solid). (b) Rating data  $A_{KK}(x)$  of Krumhansl and Kessler (1982) (dotted) and quantum probability kernel Eq. (8) (solid). Both for C major context.

The two parameters  $a_0, a_4$  are necessarily obtained from two interpolation equations

$$\begin{aligned}\gamma(0) &= 0 \\ \gamma(\pi) &= \frac{\pi}{2},\end{aligned}$$

i.e. the tonic should not be deformed while the tritone receives maximal deformation, as reflected by Fig. 3(a). Note that we do not perform a least-square fit for the parameters by minimizing some error functional. The parameters are fixed by the constraint that the deformation function should vanish at C and assume a maximum at F#. This leads to the parsimonious model

$$\gamma(x) = \frac{\pi}{2} - \frac{(x - \pi)^4}{2\pi^3}. \quad (17)$$

We plot the original Krumhansl and Kessler (1982) data and the quantum probability density kernel (8) of the deformation model (13) in Fig. 3(b) (beim Graben and Blutner 2017).

At this point, it is useful to ask for the connection between the deformation model and the hierarchical model. As one sees from Fig. 3(b), the kernel function of static tonal attraction assigns the maximum value to the target

tone C. The two neighbors on the circle of fifth, i.e., G and F, get an attraction value that is about half of it. The attraction values of all other tones is very low such that we can neglect them. Hence, when we construct the attraction profiles for a certain context given by a triad (say CEG), we get an approximate reconstruction of the hierarchic model. The three tones of the triad (CEG) get a very high value; C and G a bit higher than E because of the discrete convolution in Eq. (11). Next, the neighbors of the triadic tones (C'G,F vs. G'D,C vs. E'B,A) are all diatonic tones and get an attraction of about 50%. Hence, we can account for all levels of the hierarchic model shown in Tab. 2 besides the octave level (resulting in 4 different degrees of attraction).<sup>4</sup>

### 3.1.5. Asymmetric deformation

The mirror symmetry of the spatial deformation model against the tritone  $F\sharp$  leads to crucial problems when accounting for the differences between major and minor modes. So far, we considered the conception of static and dynamic attraction only. However, in cognitive music theory some other basic conceptions have been discussed including the idea of graded consonance/dissonance. According to Parncutt (1989), the degree of (musical) consonance of a chord is related to the distribution of potential root tones of a chord. Hereby, the root tone of a chord can be seen as the tone with maximal static attraction given the chord as musical context. In cases with a single, incisive root tone, the chord sounds more consonant than in cases where several root tones compete against each other. Formally, we express the degree of chordal consonance as the static attraction value  $p_C(x)$  [Eq. (11)] of the (root) tone with maximum attraction after normalizing the attraction profile (i.e., the attraction values of the 12 tones sum up to 1).

Recently, Johnson-Laird et al. (2012) investigated chords including major triads (CEG), minor triads ( $CE\flat G$ ), diminished triads ( $CE\flat G\flat$ ), and augmented triads ( $CEG\sharp$ ). Table 6 in Sect. 4.1 shows the empirical ratings of

---

<sup>4</sup> A more sophisticated analysis by means of harmonic analysis, that will be published elsewhere, reveals that the Hilbert space of our deformed quantum model is infinite-dimensional in contrast to the two-dimensional case of the free quantum model discussed in Sect. 3.1.2.

the chord's consonance. Clearly, the major chords exhibit the highest degree of consonance followed by the minor chords. Further, the diminished chords are ranked lower and, at the bottom, we (surprisingly) find the augmented chords. It is not difficult to see that the hierarchic model and the symmetric deformation model predict the same degrees of consonance for major and minor chords.

In order to further improve the predictive power of our quantum deformation model, we consider an asymmetric deformation polynomial of fourth order

$$\gamma(x) = a_0 + a_1(x - \pi) + a_2(x - \pi)^2 + a_3(x - \pi)^3 + a_4(x - \pi)^4, \quad (18)$$

where both, the linear term with coefficient  $a_1$  and the cubic term with coefficient  $a_3$  break the mirror-symmetry against the tritone  $F\sharp$ . As above, we demand that the tonic  $x = 0 \cong 2\pi$  is not deformed. This leads to two interpolation equations

$$\begin{aligned} \gamma(0) &= 0 \\ \gamma(2\pi) &= 0, \end{aligned}$$

allowing the elimination of two coefficients, e.g.  $a_3, a_4$ :

$$\gamma(x) = a_0 + a_1(x - \pi) + a_2(x - \pi)^2 - \frac{a_1}{\pi^2}(x - \pi)^3 - \frac{a_0 + a_2\pi^2}{\pi^4}(x - \pi)^4. \quad (19)$$

The remaining coefficients receive a straightforward interpretation as intercept:  $a_0$ , skewness:  $a_1$ , and steepness:  $a_2$  (for moderate values). Equation (19) describes the symmetric deformation (17) under the choice  $a_0 = \pi/2, a_1 = a_2 = 0$ .

We fit both parameters  $a_1$  and  $a_2$ , after inserting (19) with the default values above into the convolution (11), on the C major data set of Krumhansl and Kessler (1982) and obtain  $a_1 = -0.14, a_2 = 0.01$  ( $r = 0.982$ ). Finally, we compare our results with those of Johnson-Laird et al. (2012) for C major and C minor triads, and for diminished triads and augmented triads, respectively. The results are presented in section 4.1.2, Tab. 6.

### 3.2. Dynamic tonal attraction

In this subsection we develop a quantum model based on a deformation of cosine similarity along the circle of fifths for the dynamic tonal attraction experiment of Woolhouse (2009). This model is motivated by Woolhouse’ (2009, 2010) interval cycle proximity measure that is described in the next section 3.2.1. Note that dynamic attraction has also successfully been described by Bayesian statistical modeling and Gaussian Markov chains trained on large musical corpora (Temperley 2007, 2008).

#### 3.2.1. Interval cycle model

In recent research, Woolhouse (2009), Woolhouse and Cross (2010), and Woolhouse (2012) have proposed to explain dynamic tonal attraction in terms of interval cycles. The basic idea is that the dynamic attraction between two pitches is proportional to the number of times the interval spanned by the two pitches must be multiplied by itself to produce some whole number of octaves. Assuming twelve-tone equal temperament, the *interval-cycle proximity (ICP)* of an interval  $j \in \mathbb{Z}_{12}$  can be defined as the smallest positive number  $n$  such that the product with the interval length (i.e. the number of semitone steps spanned by the interval) is a multiple of twelve (i.e. the maximal interval length). More formally, let  $j \in \mathbb{Z}_{12}$  be an interval on the chroma circle. The ICP  $n = \text{icp}(j)$  is defined as the smallest integer  $n \in \mathbb{N}$ , such that

$$nj = 0 \pmod{12} \tag{20}$$

i.e. for a given  $j$  one looks for the actually smallest  $m \in \mathbb{N}$  such that  $nj = 12m$ , which which eventually gives

$$\text{icp}(j) = \frac{12m}{j}. \tag{21}$$

The following Tab. 3 lists the interval-cycle proximities for all intervals spanned by a given length. For example, one can see that the ICP of the tritone ( $j = 6$ ) is 2 and the ICP of the fifth ( $j = 7$ ) is 12. This has the plausible consequence that, relative to a root tone, the fifth has higher tonal attraction than the tritone.

interval $j$	0	1	2	3	4	5	6	7	8	9	10	11	12
$\text{icp}(j)$	1	12	6	4	3	12	2	12	3	4	6	12	1

Table 3: Interval cycle proximity (ICP) on chroma circle.

Two particular values of ICP are worth to be mentioned. Relative to the root, the semitone step (the minor second) receives the highest possible  $\text{icp}(1) = 12$ , while the full-tone step (the major second) assumes its half,  $\text{icp}(2) = 6$ . This fundamental relation, preferring small intervals in melodic dynamics against larger transitions is substantial for Western music (Curtis and Bharucha 2009, Krumhansl et al. 2000, Narmour 1992, Temperley 2008) and should be maintained in any alternative proposal to the IC model, such as in our quantum model below.

ICP exhibits two interesting symmetries. First, it is obviously invariant under reflection against the tritone  $j = 6$ , therefore  $\text{icp}(j) = \text{icp}(12 - j)$ . Second, it is invariant under the transition from the chroma circle to the circle of fifths and vice versa (Woolhouse and Cross 2010):  $\text{icp}(j) = \text{icp}(7j \bmod 12)$ . As a consequence, ICP assigns the highest value 12 to the minor second ( $j = 1$ ) and to the fourth ( $j = 5$ ). We may thus represent our wave functions alternatively either at the chroma circle, or at the circle of fifths. ICP are plotted along the chroma circle in Fig. 4(b) as the dotted curve.

### 3.2.2. Deformation model

In order to construct a quantum deformation model of the dynamic tonal attraction data of Woolhouse (2009) we realize that a symmetric fourth-order polynomial is not sufficient to model ICP which we though consider a good phenomenal working model for the resolution of chords into single tones, despite ongoing discussions (Quinn 2010). Therefore, we chose the next possible model class of symmetric sixth-order polynomials. We try to interpolate

$$\gamma(x) = a_0 + a_2(x - \pi)^2 + a_4(x - \pi)^4 + a_6(x - \pi)^6 \quad (22)$$

to the transformed and rescaled ICP (cf. Eq. (15))

$$\gamma(x) = \arccos \sqrt{\frac{\text{icp}(x) - 1}{11}}. \quad (23)$$

Equation (23) is ambiguous with respect to the sign of the square root. Taking only the positive square root of ICP into account, involves zeros of  $\gamma(x)$  with multiplicities larger than one, thereby generating a highly fluctuating function which prevents interpolation by a sixth-order polynomial. Thus, we avoid this ambiguity by a smoothing function  $\sigma(j)$  tabulated in Tab. 4.

interval $j$	0	1	2	3	4	5	6	7	8	9	10	11	12
$\sigma(j)$	-1	1	1	1	1	1	-1	1	1	1	1	1	-1

Table 4: Smoothing function  $\sigma$  forcing simple zeros of the ICP deformation.

The smoothing function  $\sigma$  assigns negative values to the unison ( $j = 0$ ), to the tritone ( $j = 6$ ) and to the octave ( $j = 12$ ) and positive values to all other intervals. Consequently, the zeros of  $\gamma(x)$  at the minor second ( $j = 1$ ) and the fourth ( $j = 5$ ) become simple zeros, with positive slope for  $j = 1$  and negative slope for ( $j = 5$ ), such that the graph of  $\gamma$  traverses the  $x$ -axis, thus reducing the complexity of the interpolation. For the values tabulated in Tab. 4,  $\gamma(x)$  can be interpolated with a symmetric fourth-order polynomial. Figure 4(a) shows the resulting function  $\gamma(x)/\sigma(x)$  in black.

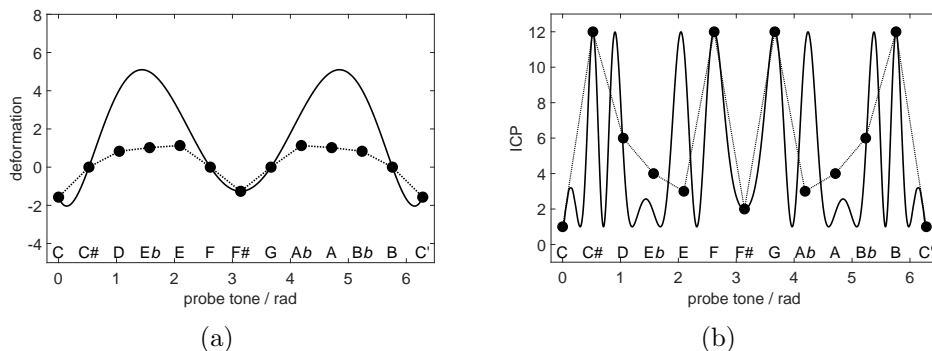


Figure 4: Optimal deformation of the cosine similarity profile for dynamic tonal attraction. (a) Transformed ICP data (23) along the chroma circle (dotted), deformation function (24) (solid). (b) ICP (dotted) and quantum deformation model (solid).

Instead of rigorously modeling the interval cycle model, we use it more as a guideline for our quantum model. Therefore, our model should at least share three important features with ICP: It should prefer small intervals

$j = 1, 2$  and it should respect the symmetries of ICP. This choice already fixes two intervals for our interpolation, namely the zeros of the transformed ICP  $\gamma$  at  $j = 1, 5$ , where the cosine similarity function (13) should not be deformed at all. For the third and fourth interpolation points, we select as in Sect. 3.1.3 the tonic at  $j = 0$  and the tritone at  $j = 6$  as the symmetry center. Then, the four parameters  $a_0, a_2, a_4, a_6$  are necessarily (without any fit) obtained from four interpolation equations

$$\begin{aligned}\gamma(0) &= -\frac{\pi}{2} \\ \gamma\left(\frac{\pi}{6}\right) &= 0 \\ \gamma\left(\frac{5\pi}{6}\right) &= 0 \\ \gamma(\pi) &= -\arccos 11^{-\frac{1}{2}}.\end{aligned}$$

The result is the parsimonious model

$$\begin{aligned}\gamma(x) &= -\arccos 11^{-\frac{1}{2}} - \frac{125\pi - 147994 \arccos 11^{-\frac{1}{2}}}{3850\pi^2}(x - \pi)^2 + \\ &+ \frac{2340\pi - 171864 \arccos 11^{-\frac{1}{2}}}{1925\pi^4}(x - \pi)^4 - \frac{3240\pi - 99792 \arccos 11^{-\frac{1}{2}}}{1925\pi^6}(x - \pi)^6.\end{aligned}\tag{24}$$

We plot the original ICP (21) and the quantum probability density (8) of the deformation model (24) Fig. 4(b). Apparently, the kernel resulting from (24) displays some fluctuations over the chroma circle. Interestingly, although the deformation was interpolated only at four intervals C, C $\sharp$ , F and F $\sharp$  in Fig. 4(a), the resulting attraction profile agrees with ICP also at the interval D which is crucial for predicting the ratings of the major second interval. However, or interpolation substantially deviates from ICP at minor and major thirds Eb and E.

## 4. Results

This section summarizes the results of our quantum models for tonal attraction which will be compared with traditional models of Lerdahl (1988,

1996), Krumhansl and Kessler (1982) for the static and Woolhouse (2009), Woolhouse and Cross (2010) for the dynamic attraction data.

#### 4.1. Static tonal attraction

First, we consider a symmetric deformation function as derived in Sect. 3.1.4.

##### 4.1.1. Symmetric deformation

Computing the quantum probabilities (8) for the free model gives the results in Fig. 5. Figure 5(a) shows the agreement of the rescaled quantum probability densities with the Krumhansl and Kessler (1982) data for C major, and Fig. 5(b) for C minor. The dotted curves display the results of the Krumhansl and Kessler (1982) experiment, arranged along the circle of fifths. The dashed curves show the continuous quantum probability density  $p_C(x)$  [Eq. (11)] obtained from the convolution of the kernel function  $p(x)$  (8) of the free pure state wave function  $\psi(x)$  [Eq. (3)] over the major triad context CEG (a) and the minor triad context C**E**bG (b). The solid curves display  $p_C(x)$  discretely sampled across the circle of fifths.

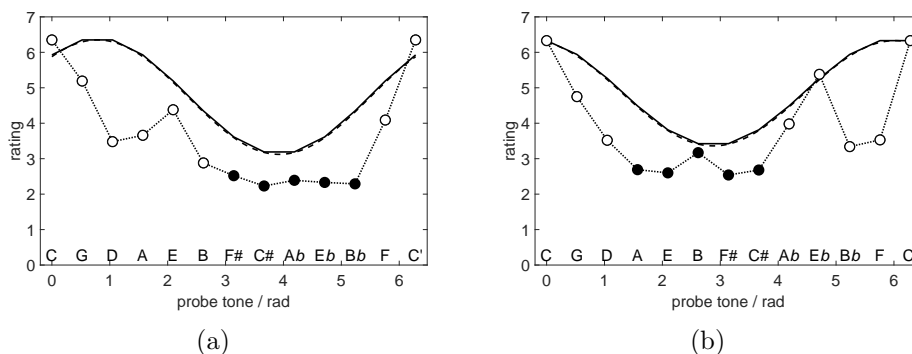


Figure 5: Free quantum (cosine similarity) model for static tonal attraction. Dotted with bullets: rating data  $A_{KK}(x)$  of Krumhansl and Kessler (1982) against radian angles at the circle of fifths, dashed: continuous mixed state model  $p_C(x)$  [Eq. (11)]. (a) For C major context. (b) For C minor context. Solid:  $p_C(x)$  after discrete sampling across the circle of fifths. Open bullets indicate scale (diatonic) tones; closed bullets denote non-scale (chromatic) tones.

In Fig. 6 we present the results of modeling the Krumhansl and Kessler (1982) data (dotted) with the quantum deformation approach [Eqs. (13), (17)]. Computing the mixed state quantum probabilities  $p_C(x)$  as convolutions of  $p(x)$  [(8)] over the major triad context CEG (a) and the minor triad context C**E**bG (b) [Eq. (11)] gives the dashed curves. The solid curves display  $p_C(x)$  after discrete sampling.

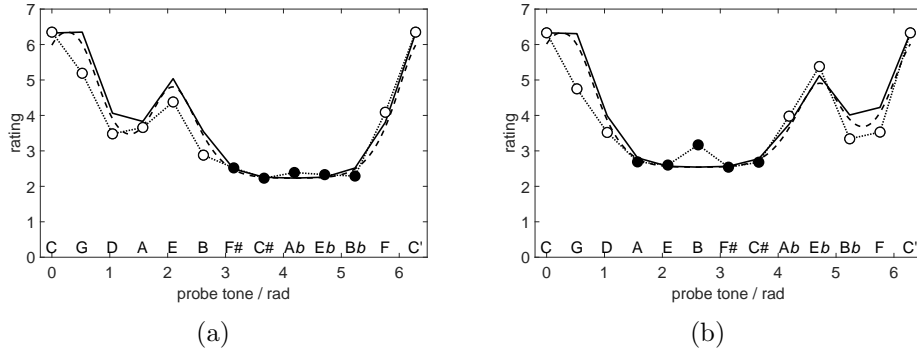


Figure 6: Quantum deformation model for static tonal attraction. Dotted with bullets: rating data  $A_{KK}(x)$  of Krumhansl and Kessler (1982) against radian angles at the circle of fifths, dashed: mixed state model  $p_C(x)$  [Eq. (11)]. (a) For C major context. (b) For C minor context. Solid:  $p_C(x)$  after discrete sampling across the circle of fifths. Open bullets indicate scale (diatonic) tones; closed bullets denote non-scale (chromatic) tones.

Obviously, the mixed state quantum deformation model tracks the experimental data almost perfectly. In particular it is able to unveil the different levels of the hierarchical model: the tonic receives maximal attraction, followed by the fifth, by the third, and eventually by the remaining diatonic scale tones. However, the model does not capture the slight asymmetry between major and minor modes in the data.

Carrying out a correlation analysis between model and data yields the results in Tab. 5.

	hierarchical model	free model		sym. deformation model	
		pure	mixed	pure	mixed
C major	0.98	0.70	0.78	0.89	0.97
C minor	0.95	0.68	0.72	0.80	0.93

Table 5: Correlation coefficients  $r$  of four discussed models for static tonal attraction with Krumhansl and Kessler (1982) data. All error probabilities are significantly below 0.05.

The free cosine similarity model already accounts for about  $r^2 = 50\%$  of the data’s variance for pure quantum states and slightly improves for mixed quantum states convolved over contextual triads. The deformation model performs much better for pure quantum states and does as good as the hierarchical model based on the generative theory of tonal music. Hence, we conclude that our quantum model is able to explain the experimental results on static tonal attraction using a parsimonious approach.

This contrasts with the hierarchical model in methodological and empirical respects. As outlined in Sect. 3.1.1, the hierarchical model stipulates all five levels of description that are essential for predicting tonal attraction ratings. In this sense, the hierarchical model lacks explanatory power. Our deformation model, however, only has to stipulate the triadic level of the hierarchical model. This level is used for calculating the discrete convolution (11) of the deformation kernel (8). From this, the entire major and minor scales are rendered. As discussed in Sect. 3.1.3, the deformation ansatz derives all levels of the hierarchic model, besides the octave level, from the triadic context together with the mixing conjecture and does not require any further stipulation. Thus, our model parsimoniously outperforms the hierarchical model in terms of explanatory power.

#### 4.1.2. Asymmetric deformation

Finally, we present the results for the asymmetric deformation model from Sect. 3.1.5 in Tab. 6. The asymmetric quantum model is able to explain the correct consonance ranking of major (CEG), minor (CE $\flat$ G), diminished (CE $\flat$ G $\flat$ ), and augmented triads (CEG $\sharp$ ), respectively (Johnson-Laird et al. 2012). For the hierarchical model the correlation is  $r = 0.93$  ( $p = 0.07$ ), for the asymmetric deformation model we have  $r = 0.95$  ( $p = 0.05$ ).

	emp. consonance	hier. model	asym. deformation model
major	5.33	0.49	0.54
minor	4.59	0.49	0.52
diminished	3.11	0.34	0.36
augmented	1.74	0.33	0.34

Table 6: Empirical consonance ratings and model predictions for common triads. The predictions of the models concern the strength of strongest static attraction using normalized attraction profiles.

Summarizing, we consider a case of symmetry breaking in cognitive musicology, breaking the mirror symmetry of the tonal attraction kernel in analogy to Parncutt (2011). In this way, we overcome some weaknesses of the classical attraction model based on tonal hierarchies, which cannot account for the differences between major and minor modes. Consequently, we get a suitable model not only for static attraction profiles but also for graded consonance/dissonance. The ability for unification — grasping different phenomena in a systematic way — is one of the trademarks of quantum theory, which is correspondingly apparent in the domain of quantum cognition as well.

#### 4.2. Dynamic tonal attraction

Here, we present the results of modeling the Woolhouse (2009) data with the quantum deformation model that was somewhat motivated by the interval cycle model. Computing the probability densities (11) for five contexts gives the results in Fig. 7. Figure 7(a) shows the agreement of the model with the Woolhouse (2009) data for C major, (b) for C minor, (c) for the dominant seventh, (d) for French sixth, and (e) for half-diminished seventh. The dotted curves present the original results of the Woolhouse (2009) experiment. The dashed curves display the continuous quantum probability density  $p_C$  obtained from the mixture of pure states over all context tones in the respective chords: major triad CEG (a), minor triad CE♭G (b), dominant seventh CEGB♭ (c), French sixth CEG♭B♭ (d), and half-diminished seventh CE♭G♭B♭ (e).

Finally, we also deliver our model’s prediction (f) for the famous “Tristan

chord” from Richard Wagner’s opera *Tristan und Isolde* (1860). Following Woolhouse (2012), the tension induced by the “Tristan chord”  $E\flat FG\sharp B$ , which is further strengthened by an intervening French sixth  $E\flat FAB$ , betokened by a single A, is eventually resolved by the chord  $EG\sharp DB\flat$ .<sup>5</sup>

---

<sup>5</sup> At the moment, no empirical data are available for the “Tristan chord”.

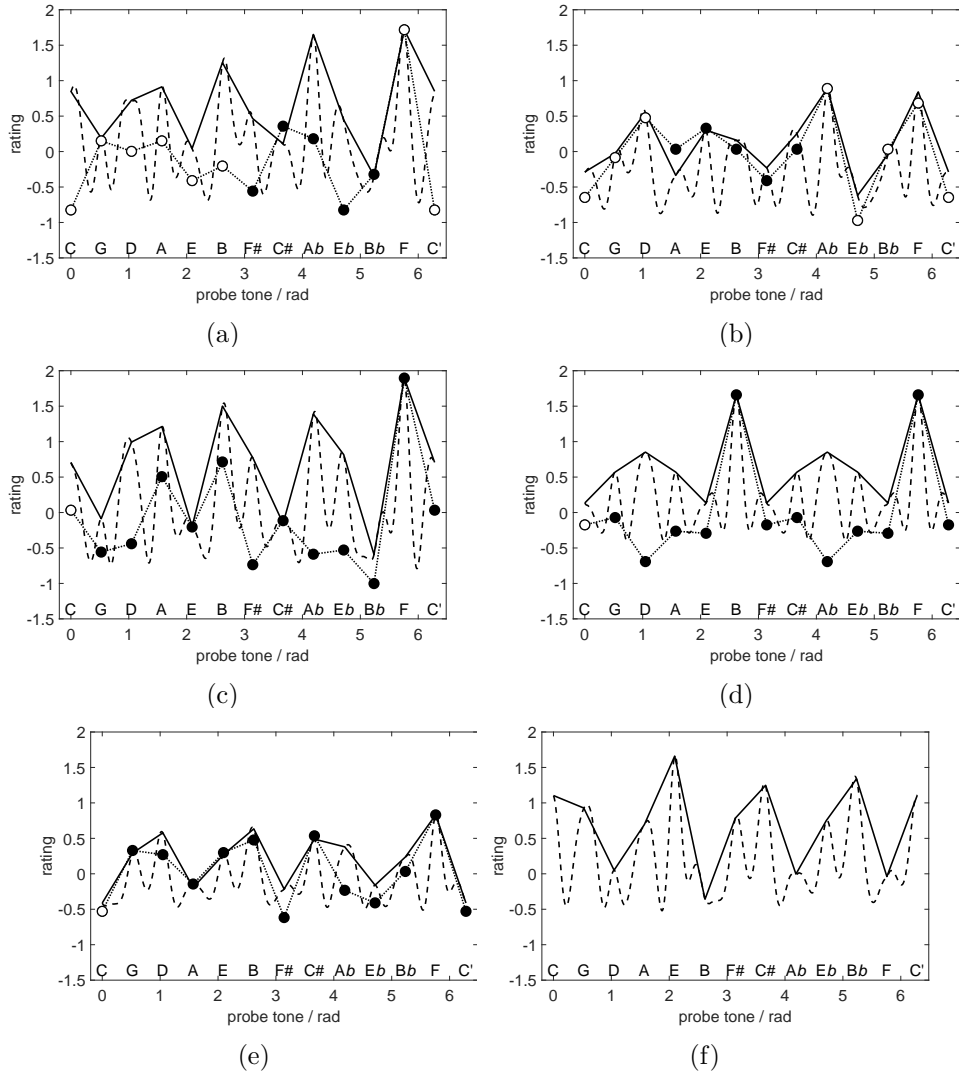


Figure 7: Quantum deformation model for dynamic tonal attraction data. Dotted with bullets: Rating data  $A_W(x)$  of Woolhouse (2009) against radian angles at the circle of fifths. Dashed: quantum probability density  $p_C(x)$  of the mixed state model (11). (a) For C major context. (b) For C minor context. (c) For dominant seventh. (d) For French sixth. (e) For half-diminished seventh. (f) For “Tristan chord”. Solid: mixed state density after sampling along the circle of fifths.

The mixed state quantum deformation model assigns highest attraction values to F, Ab, B, A, and C (in this order) [Fig. 7(a)]. This is consistent

with the interpretation of the C major context as the dominant of F major, containing F, A and C. Another possibility is the interpretation of the C major context as the subdominant of G major, comprised by G, B, and D. However, the agreement with model and data is confined to F, G, B $\flat$ , and C $\sharp$ . For C minor shown in [Fig. 7(b)], the model almost perfectly agrees with the experimental results: highest attraction values are assigned to A $\flat$ , F, and D. The model conforms also with music-theoretic predictions, resolving either the dominant of F minor into its tonic F A $\flat$  C, or the subdominant of G minor into G B $\flat$  D. Also for the dominant seventh [Fig. 7(c)] the model correctly predicts F as the most likely resolution. For E and C $\sharp$  model and data agree quite well. The French sixth context [Fig. 7(d)] correctly predicts resolution at B and F, but there is not much correlation with other data points. This is different for the half-diminished seventh plotted in [Fig. 7(e)], where the model curve tracks the experimental data quite well, besides A $\flat$ . Figure 7(f) demonstrates a remarkable performance of our model predicting the resolution of the ambiguous “Tristan chord”. The predicted attraction rate is maximal at E and B $\flat$ , those tones that belong to the resolving chord E G $\sharp$  D B $\flat$ . Interestingly, a similar analysis (not shown) for the intervening French sixth also yields large attraction values for E and B $\flat$ , which are thereby further enhanced. In addition, the French sixth also increases attraction rates for the resolving G $\sharp$  and D. The ambiguity of the “Tristan chord” is reflected in our model by also predicting high attractions for C and C $\sharp$ .<sup>6</sup>

The quality of our model is assessed by the regression analysis presented in Tab. 7.

	IC model	deformation model
C major	0.69	0.44
C minor	0.76	0.93
dominant seventh	0.76	0.65
French sixth	0.79	0.76
half-diminished seventh	0.89	0.90

Table 7: Correlation coefficients  $r$  of two discussed models for dynamic tonal attraction with Woolhouse (2009) data. All error probabilities are significantly below 0.05.

<sup>6</sup> We thank one reviewer for this interesting remark.

The correlation coefficients confirm the outcome of visually inspecting Fig. 7. For C minor and the half-diminished seventh our quantum model performs slightly better than the IC model of Woolhouse (2009) and Woolhouse and Cross (2010). Moreover, our model predicts the resolution of the “Tristan chord” (Woolhouse 2012). However, the main advantage of the quantum deformation model goes beyond the Woolhouse model and is able describing both the static and the dynamic attraction data.

## 5. Discussion

Tonal attraction is an important issue in the psychology of music. In this study, we have discussed two kinds of tonal attraction as investigated by probe tone experiments. Static tonal attraction refers to the stability or instability of tones or chords in a certain context, establishing a tonal key. By contrast, dynamic tonal attraction reflects the predictability of tones or chords continuing a preestablished melodic or harmonic context (Temperley 2008). In the paradigm of probe tone experiments (Krumhansl and Shepard 1979, Krumhansl 1979), static and dynamic attraction are investigated by means of different kinds of instructions: On the one hand, in a static attraction experiment, subjects are asked to rate how well a presented probe tone fits to a priming context (Krumhansl and Kessler 1982). In a dynamic attraction experiment, on the other hand, subjects are asked to rate how well a given probe tone completes or resolves the priming context, both melodically or harmonically (Woolhouse 2009).

It was the aim of this study to integrate structural and probabilistic theories of computational music theory into a unified framework. On the one hand, structural accounts such as the generative theory of tonal music are guided by principle musicological insights about the intrinsic symmetries of Western tonal music (Lerdahl and Jackendoff 1983, Lerdahl 1988, 1996). On the other hand, probabilistic accounts such as Bayesian models or Gaussian Markov chains are able to describe melodic progression through statistical correlations in large music corpora (Temperley 2007, 2008). Here, we argued that quantum approaches to music cognition are able to unify symmetry and (quantum) probability in a single framework for data from static and dynamic attraction experiments.

In a first attempt to describing the static attraction data of Krumhansl and Kessler (1982), we realized that simply rearranging the data points according to the universal circle of fifths, instead of increasing physical pitch frequency, revealed a systematic pattern of periodic attraction: tones close to the tonic are more attractive than tones in the vicinity of the tritone. Since this periodicity could be expressed as a cosine similarity measure, often used in quantum cognition models of similarity judgements (Pothos et al. 2013, Pothos and Trueblood 2015), we were led to the formulation of a quantum model of tonal attraction by means of a “wave function” defined over the circle group as “configuration space” which includes the circle of fifths as a subgroup. An important insight from our free quantum model is that its Hilbert space is essentially two-dimensional which proves its equivalence with an earlier qubit model proposed by Blutner (2015).

In order to improve our free model, we developed a “deformation” quantum model, still based on cosine quantum similarity, but introducing a deformation of interval lengths over the circle of fifths. We described this deformation function as a symmetric polynomial of fourth order, and determined its parameters from two necessary interpolation conditions, saying that the tonic should not be deformed at all, while the tritone receives maximal deformation. The quantum wave functions of our approach can be interpreted as musical Gestalts in the sense of Gestalt psychology (Köhler 1969).

For assessment of the tonal attraction of complex priming stimuli such as chords or cadences, we followed a suggestion recently conjectured by Woolhouse and Cross (2010) and exploited by Blutner (2015) to compute the discrete convolution of a kernel function, the quantum probability obtained from the squared wave function, and a uniform distribution over all context tones. As contexts, we assumed the tonic triads of the C major and C minor keys for static attraction, here. This is similar to the hierarchical model of Lerdahl (1988, 1996), where the tonic triad comprises level C in the hierarchy. As a result, our model precisely reproduced the experimental data with comparable statistical performance as the hierarchical model. However, while the hierarchical model has to stipulate the existence of all five levels in the hierarchy, our model only refers to the C level. The other levels A – E required by the hierarchical model are deduced from our model. Therefore, our quantum model parsimoniously outperforms the hierarchical model of static attraction with respect to explanatory power.

However, the symmetric deformation model for static tonal attraction does not correctly describe the observed asymmetry between major and minor modes in the Krumhansl and Kessler (1982) data. This is also a problem for the hierarchical model as well. We therefore additionally presented an asymmetric deformation model that breaks the mirror symmetry against the tritone. Fitting two free parameters of this model to the major context, we were able to achieve substantial improvement also for minor keys and an understanding for the different degrees of consonance for major, minor, diminished, and augmented chords.

For dynamic tonal attraction we devised a similar quantum model based on a sixth-order polynomial deformation. This construction was guided by the interval cycle model of Woolhouse and Cross (2010) and Woolhouse (2009) and in agreement to related models that prefer small intervals over longer ones for melodic and harmonic dynamics (Curtis and Bharucha 2009, Krumhansl et al. 2000, Narmour 1992, Temperley 2008). Our model performed comparably well as the ICP model in a regression analysis. Interestingly, our model confirms predictions about the resolution of context chords based on musical harmony theory with good accuracy.

Finally, we address the possible relevance of our work to the cognitive neuroscience of music perception. The behavioral findings of Krumhansl and Kessler (1982) and Woolhouse (2009) have been supported by neuropsychological experiments in the event-related brain potential (ERP) (Granot and Hai 2009, Limb 2006) and in the functional magnetic resonance (fMRI) paradigms (Durrant et al. 2007, Janata et al. 2002, Koelsch et al. 2002, Limb 2006, Vaquero et al. 2016). The first three fMRI studies used melodies with harmonic modulation from one key into another key as stimuli and reported significant anatomical differences for key changes. In particular, Janata et al. (2002), who carried out a regression analysis of fMRI data with self-organized maps trained upon the third torus as tonal space (Janata et al. 2002, Purwins et al. 2007), made the strong claim that the rostromedial prefrontal cortex exhibits a neural tonotopic representation of the third torus.

## 6. Conclusions

This study applies methods from the quantum cognition framework to tonal attraction. In probe tone experiments, music psychologists measure the likelihood of chromatic probe tones relative to a priming context. Depending on the particular instruction, the subject’s ratings assess either the degree of fit between a probe tone and a key context (static attraction), or the degree of predictability of a probe tone given a preceding context (dynamic attraction). A first attempt reveals that tonal attraction correlates with quantum similarity between tones across the universal circle of fifths. Deforming the distances between tones leads to two quantum wave functions, one for static attraction, the second for dynamic attraction. We compute their attraction profiles for tonic contexts and compare them with predictions of the hierarchical model in the static case and of the interval cycle model for the dynamic case. Our parsimonious quantum models provide precise and rigorous results with great explanatory power.

## Acknowledgments

We thank Maria Mannone, Serafim Rodrigues and Günther Wirsching for valuable comments on an earlier version of the manuscript.

## References

## References

- Balzano, G. J. (1980). The group-theoretic description of 12-fold and microtonal pitch systems. *Computer Music Journal*, 4(4):66 – 84.
- beim Graben, P. and Blutner, R. (2017). Toward a gauge theory of musical forces. In de Barros, J. A., Coecke, B., and Pothos, E., editors, *Quantum Interaction. 10th International Conference (QI 2016)*, volume 10106 of *LNCS*, pages 99 – 111. Springer, Cham.

- Blutner, R. (2015). Modelling tonal attraction: tonal hierarchies, interval cycles, and quantum probabilities. *Soft Computing*, pages 1 – 19.
- Blutner, R. and beim Graben, P. (2016). Quantum cognition and bounded rationality. *Synthese*, 193:3239 – 3291.
- Busemeyer, J. R. and Bruza, P. D., editors (2012). *Quantum Models of Cognition and Decision*. Cambridge University Press.
- Curtis, M. E. and Bharucha, J. J. (2009). Memory and musical expectation for tones in cultural context. *Music Perception: An Interdisciplinary Journal*, 26(4):365 – 375.
- Durrant, S., Miranda, E. R., Hardoon, D., Shawe-Taylor, J., Brechmann, A., and Scheich, H. (2007). Neural correlates of tonality in music. In *Proceedings of the NIPS Conference Workshop on Music, Brain & Cognition*.
- Granot, R. Y. and Hai, A. (2009). Electrophysiological evidence for a two-stage process underlying single chord priming. *NeuroReport*, 20(9).
- Janata, P. (2007). Navigating tonal space. In Selfridge-Field, E. and Hewlett, W. B., editors, *Tonal Theory for the Digital Age*, volume 15 of *Computing in Musicology*, pages 39 – 50. MIT Press, Cambridge (MA).
- Janata, P., Birk, J. L., Horn, J. D. V., Leman, M., Tillmann, B., and Bharucha, J. J. (2002). The cortical topography of tonal structures underlying western music. *Science*, 298(5601):2167 – 2170.
- Johnson-Laird, P. N., Kang, O. E., and Leong, Y. C. (2012). On musical dissonance. *Music Perception: An Interdisciplinary Journal*, 30(1):19 – 35.
- Koelsch, S., Gunter, T. C., von Cramon, D. Y., Zysset, S., Lohmann, G., and Friederici, A. D. (2002). Bach speaks: a cortical “language-network” serves the processing of music. *NeuroImage*, 17(2):956 – 966.
- Köhler, W. (1969). *The Task of Gestalt Psychology*. Princeton University Press, New Jersey.
- Krumhansl, C. L. (1979). The psychological representation of musical pitch in a tonal context. *Cognitive Psychology*, 11(3):346 – 374.

- Krumhansl, C. L. and Cuddy, L. L. (2010). A theory of tonal hierarchies in music. In Jones, M. R., Fay, R. R., and Popper, A. N., editors, *Music Perception*, Springer Handbook of Auditory Research, pages 51 – 87. Springer, New York.
- Krumhansl, C. L. and Kessler, E. J. (1982). Tracing the dynamic changes in perceived tonal organization in a spatial representation of musical keys. *Psychological Review*, 89(4):334 – 368.
- Krumhansl, C. L. and Shepard, R. N. (1979). Quantification of the hierarchy of tonal functions within a diatonic context. *Journal of Experimental Psychology: Human Perception and Performance*, 5(4):579.
- Krumhansl, C. L., Toivanen, P., Eerola, T., Toiviainen, P., Järvinen, T., and Louhivuori, J. (2000). Cross-cultural music cognition: Cognitive methodology applied to North Sami yoiks. *Cognition*, 76(1):13 – 58.
- Lerdahl, F. (1988). Tonal pitch space. *Music Perception: An Interdisciplinary Journal*, 5:315 – 350.
- Lerdahl, F. (1996). Calculating tonal tension. *Music Perception: An Interdisciplinary Journal*, 13(3):319 – 363.
- Lerdahl, F. (2015). Concepts and representations of musical hierarchies. *Music Perception: An Interdisciplinary Journal*, 33(1):83 – 95.
- Lerdahl, F. and Jackendoff, R. (1983). *A Generative Theory of Tonal Music*. MIT Press, Cambridge (MA).
- Limb, C. J. (2006). Structural and functional neural correlates of music perception. *The Anatomical Record Part A: Discoveries in Molecular, Cellular, and Evolutionary Biology*, 288A(4):435 – 446.
- Mannone, M. (2018). Knots, music, and DNA. *Journal of Creative Music Systems*, 2(2).
- Mannone, M. and Compagno, G. (2013). Characterization of the degree of musical non-Markovianity. arXiv:1306.0229 [physics.data-an].
- Mannone, M. and Mazzola, G. (2015). Hypergestures in complex time: Creative performance between symbolic and physical reality. In Collins, T.,

- Meredith, D., and Volk, A., editors, *Proceedings of the 5th International Conference on Mathematics and Computation in Music (MCM 2015)*, pages 137 – 148, Cham. Springer.
- Mazzola, G. (1990). *Geometrie der Töne*. Birkhäuser, Basel.
- Mazzola, G. (2002). *The Topos of Music: Geometric Logic of Concepts, Theory, and Performance*. Birkhäuser, Basel.
- Mazzola, G., Mannone, M., and Pang, Y. (2016). *Cool Math for Hot Music*. Computational Music Science. Springer, Cham.
- Milne, A. J., Laney, R., and Sharp, D. B. (2015). A spectral pitch class model of the probe tone data and scalic tonality. *Music Perception: An Interdisciplinary Journal*, 32(4):364 – 393.
- Milne, A. J., Sethares, W. A., Laney, R., and Sharp, D. B. (2011). Modelling the similarity of pitch collections with expectation tensors. *Journal of Mathematics and Music*, 5(1):1 – 20.
- Narmour, E. (1992). *The Analysis and Cognition of Melodic Complexity: The Implication-Realization Model*. University of Chicago Press, Chicago (IL).
- Parncutt, R. (1989). *Harmony: A Psychoacoustical Approach*. Springer, Berlin.
- Parncutt, R. (2011). The tonic as triad: Key profiles as pitch salience profiles of tonic triads. *Music Perception: An Interdisciplinary Journal*, 28(4):333 – 366.
- Pothos, E. M. and Busemeyer, J. R. (2013). Can quantum probability provide a new direction for cognitive modeling? *Behavioral and Brain Sciences*, 36:255 – 274.
- Pothos, E. M., Busemeyer, J. R., and Trueblood, J. S. (2013). A quantum geometric model of similarity. *Psychological Review*, 120(3):679 – 696.
- Pothos, E. M. and Trueblood, J. S. (2015). Structured representations in a quantum probability model of similarity. *Journal of Mathematical Psychology*, 64-65:35 – 43.

- Purwins, H., Blankertz, B., and Obermayer, K. (2007). Toroidal models in tonal theory and pitch-class analysis. In Selfridge-Field, E. and Hewlett, W. B., editors, *Tonal Theory for the Digital Age*, volume 15 of *Computing in Musicology*, pages 73 – 98. MIT Press, Cambridge (MA).
- Quinn, I. (2010). On Woolhouse’s interval-cycle proximity hypothesis. *Music Theory Spectrum*, 32:172 – 179.
- Schönberg, A. (1978). *Theory of Harmony*. University of California Press, Berkeley (CA).
- Stolzenburg, F. (2015). Harmony perception by periodicity detection. *Journal of Mathematics and Music*, 9(3):215 – 238.
- Temperley, D. (2007). *Music and Probability*. MIT Press, Cambridge (MA).
- Temperley, D. (2008). A probabilistic model of melody perception. *Cognitive Science*, 32(2):418 – 444.
- v. Helmholtz, H. (1877). *On the Sensations of Tones*. Dover, New York (NY). Translated by A. J. Ellis.
- Vaquero, L., Hartmann, K., Ripollés, P., Rojo, N., Sierpowska, J., François, C., Càmarà, E., van Vugt, F. T., Mohammadi, B., Samii, A., Münte, T. F., Rodríguez-Fornells, A., and Altenmüller, E. (2016). Structural neuroplasticity in expert pianists depends on the age of musical training onset. *NeuroImage*, 126(Supplement C):106 – 119.
- Woolhouse, M. (2009). Modelling tonal attraction between adjacent musical elements. *Journal of New Music Research*, 38(4):357 – 379.
- Woolhouse, M. (2012). Wagner in the round: using interval cycles to model chromatic harmony. In Cambouropoulos, E., Tsougras, C., Mavromatis, P., and Pantiadis, K., editors, *Proceedings of the 12th International Conference on Music Perception and Cognition and the 8th Triennial Conference of the European Society for the Cognitive Sciences of Music*, pages 1142 – 1145.
- Woolhouse, M. and Cross, I. (2010). Using interval cycles to model Krumhansl’s tonal hierarchies. *Music Theory Spectrum*, 32(1):60 – 78.